

Adsorption and Epitaxy in the System Ag-Cl on Spherical Silver Crystals

R. Wilken and E. Menzel

Institut B für Physik der Technischen Universität Braunschweig,
Abteilung für Grenzflächenphysik

(Z. Naturforsch. **32a**, 1266–1274 [1977]; received August 29, 1977)

Spherical silver crystals are grown in UHV by solidification of a drop of melted material and exposed to chlorine gas with doses up to 120×10^{-6} torrsec at 20 to 60°C. In situ investigations by RHEED have shown the known structures Ag(001) $c(2 \times 2)$ and Ag(011) (2×1) and new ones ("statistical chains") on Ag(011), Ag(011) (4×1) , Ag(011) (3×1) and Ag(0*kl*) (1×1) near to Ag(011). Higher doses of chlorine gas have been applied in an other apparatus starting from 10^{-5} torr; here in situ RHEED has shown the known structures, Ag(111) $(4/3 \times 4/3)$ and other ones and finally the epitaxial connections Ag-AgCl reported earlier. Adsorption nets and epitaxy have surprising correlations in the system Ag-Cl, rarely found in other systems.

1. Introduction

The relationship between surface structures after twodimensional adsorption and threedimensional epitaxy of tarnish layers had been neglected for a long time. The reason was, perhaps, that such a correlation had been found in the past only rarely. Shortly we will give a general survey on this question, but now the positive correlations shall be reported, which have been observed between surface structures on spherical silver crystals and the crystallographic orientations of AgCl on these crystals after adsorption of chlorine gas^{1,2}. Both investigations were done by using the RHEED technique.

Adsorption structures and epitaxy depend both on the crystallographic orientations of the reacting surfaces and on their preparation. Mostly low indexed surfaces prepared in a conventional way by ion bombardement and annealing had been investigated. However, higher indexed surfaces will provide additional information which not only is of great interest by itself but also will improve the understanding of phenomena occuring on low indexed planes. Spherical shaped crystals present surfaces with all crystallographic orientations. For this investigation such crystals have been used in situ without applying any further treatment after growing them by solidification of a drop of melted material in a temperature gradient³. This surface preparation is different from the conventional one

and may be helpfull in justing and finally eliminating the influence of preparation methods. Metal crystals prepared as described have been used succesfully in other investigations⁴.

2. Epitaxy: AgCl on Spherical Ag Crystals

The crystal orientations of AgCl on spherical Ag crystals had been investigated in the past by using the RHEED technique². Chlorination was performed at 20°C in air over conc. HCl. Eight different epitaxial connections had been found. The areas of existence are indicated in Fig. 1 using the characteristic stereographic triangle. All connections have been observed again in this investigation.

As a surprising feature connection A shows a systematic tilt δ of the AgCl-lattice depending on the angular distance β between the Ag pole under investigation and Ag(011). On the Ag[100] zone circle δ varies from 0° to 10° for β increasing to 18° on Ag(012).

The epitaxial connections A, B, C, D and E had been observed earlier by Pashley⁵ on those low indexed planes which center the areas of existence of A, B, C, D and E in Figure 1.

3. Known Twodimensional Structures on Ag Induced by Chlorine

Rovida and Pratesi⁶ investigated adsorption structures of chlorine on three low indexed silver surfaces using LEED and AES. They prepared the surfaces in a conventionally way, and chlorination was performed at nearly 100°C by thermal decomposition of $\text{CH}_2\text{CH}_2\text{Cl}_2$ between 10^{-3} and 10^{-2} torr. The authors observed the structures Ag(001)

Reprint requests to Prof. Dr. E. Menzel, Institut B für Physik der Technischen Universität, Abteilung für Grenzflächenphysik, Postfach 3329, D-3300 Braunschweig.

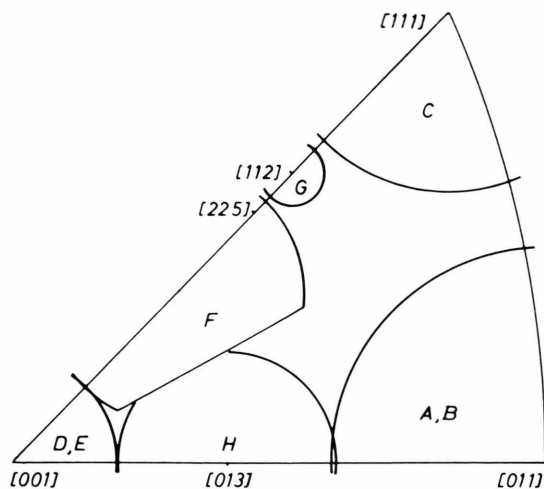


Dieses Werk wurde im Jahr 2013 vom Verlag Zeitschrift für Naturforschung in Zusammenarbeit mit der Max-Planck-Gesellschaft zur Förderung der Wissenschaften e.V. digitalisiert und unter folgender Lizenz veröffentlicht: Creative Commons Namensnennung-Keine Bearbeitung 3.0 Deutschland Lizenz.

Zum 01.01.2015 ist eine Anpassung der Lizenzbedingungen (Entfall der Creative Commons Lizenzbedingung „Keine Bearbeitung“) beabsichtigt, um eine Nachnutzung auch im Rahmen zukünftiger wissenschaftlicher Nutzungsformen zu ermöglichen.

This work has been digitalized and published in 2013 by Verlag Zeitschrift für Naturforschung in cooperation with the Max Planck Society for the Advancement of Science under a Creative Commons Attribution-NoDerivs 3.0 Germany License.

On 01.01.2015 it is planned to change the License Conditions (the removal of the Creative Commons License condition "no derivative works"). This is to allow reuse in the area of future scientific usage.

Fig. 1. Epitactic systems on silver ²

- A: Ag (011) $[100] \parallel \text{AgCl (011)} [0\bar{1}1]$
 B: Ag (011) $[100] \parallel \text{AgCl (111)} [0\bar{1}1]$
 C: Ag (111) $[0\bar{1}1] \parallel \text{AgCl (111)} [0\bar{1}1]$
 D: Ag (001) $[1\bar{1}0] \parallel \text{AgCl (001)} [100]$
 E: Ag (001) $[1\bar{1}0] \parallel \text{AgCl (111)} [1\bar{1}0]$
 F: Ag (225) $[1\bar{1}0] \parallel \text{AgCl (011)} [0\bar{1}1]$
 G: Ag (112) $[1\bar{1}0] \parallel \text{AgCl (012)} [100]$
 H: Ag (013) $[100] \parallel \text{AgCl (111)} [1\bar{1}0]$.

c(2 × 2), Ag(111) ($\sqrt{3} \times \sqrt{3}$) – 30° and Ag(011) (2 × 1) after weak chlorination and Ag(001) c(2 × 2), Ag(111) (3 × 3) and Ag(011) c(4 × 2) after stronger chlorination. Zanazzi et al.⁷ investigated and discussed Ag(001) c(2 × 2) in detail using the same technique.

4. Preparation of Ag Crystal Spheres and Their Behavior

5N silver from different supplies was used for this investigation. The material was cleaned by filing, etching did not improve the results. The crystals were processed in a RHEED apparatus (Vacuum Generators, base pressure 1×10^{-10} torr). The crystal support was fixed on a specimen manipulator. The support consisted of a pair of sheets of spectral graphite (Ringsdorff RW III, 20 ppm impurities) in contact. Heated by a stabilized d.c. current this contact acts as the main source of heat, and as a result the specimen solidifies in a defined temperature gradient parallel to the surface of the support, if the heating current is lowered.

When the silver was melted for the first time, the vacuum pressure deteriorated to 10^{-7} torr. After two further cycles of melting and solidification the pressure stabilized and did not exceed 2×10^{-9} torr during subsequent melting and solidification cycles.

The composition of the residual gas was monitored with a quadrupole gas analyzer. No unusual peak was detected during the melting phase and the peak ratio of the Ag isotopes 107 and 109 was found to correspond with the natural abundance of these isotopes.

The crystals grown on graphite have the shape of a drop of melt ("sessile drop") sitting on the support without adhesion. As a consequence of the anisotropy of free surface energy at the melting temperature the crystals show small flat areas⁸ around their (111) and (001) poles. The contour lines of these flats are egg shaped with the tip showing in the direction of solidification. The main axes of the (111) flats have angular diameters of 11° and 6°, the (001) flats have axes of 5° and 4°. Around the (111) flats there are areas with concentric terraces (diameter ca. 32°). Silver crystals grown from one supply (Heraeus 1966 "4N5") were smooth outside the (111) terraced areas at least in the sense of light optics. Crystals from another supply (Heraeus 1969 "5N") showed grooves on their (001) flats and tiny terraces also around these flats. From the present investigations and from other experiments we are lead to the assumption that all deviations from smoothness are introduced by unknown impurities. Crystals from both supplies did not show any difference with respect to the structures of adsorption and epitaxy in the system Ag-Cl.

Diffraction diagrams of 30 kV electrons taken in situ from different poles on the spherical silver crystals show always surface nets consistent with the bulk lattice. The sharp Kikuchi diagram was helpful for indexing the surface under investigation.

5. Chlorination in Cl Gas

Chlorination of the silver crystals was performed in the UHV-RHEED apparatus either immediately after the crystal had solidified or some time later.

The temperature varies between 20 °C and 60 °C. Pressured 3N chlorine gas (Merck) was used. The gas pressure was reduced to 0.1 torr by expanding the gas into a container, which was previously evacuated to a pressure of 5×10^{-9} torr. From the container, the chlorine gas was passed through a leak valve and a capillary tube ending near to the crystal. All parts were made from stainless steel. It was possible to perform electron diffraction during the chlorination process.

When the leak valve was opened, the total pressure in the vacuum chamber increased linearly with a constant rate of about 10^{-11} torr/sec from an initial value of 4×10^{-10} torr with the ion pump continuously operating. The maximal pressure was about 10^{-8} torr. Measurements with the gas analyzer in that time indicated that the peaks from carbon compounds and small spurious peaks from Cl, Cl₂, and O remained essentially constant. However, increasing signals of N, N₂ and noble gases and, with

a delay, also of O₂ appeared in the mass-spectrogram with a final ratio of nitrogen : noble gases : O₂ = 100 : 20 : 2. Since chlorine atoms do not have direct access to the gas analyzer, multiple reflections from the chamber walls are required for the atoms to reach the analyzer. From these measurements it is concluded that the chlorine atoms do not experience many reflections and reach the analyzer, but will be adsorbed at the walls generating the other gases by a desorption process. It is therefore assumed that the total pressure p is a measure for the chlorine pressure in the vicinity of the crystal. The quantity $p \times t$ represents then the exposure of the crystal to the chlorine with t being the time the leak valve was open. In order to avoid damage to the UHV apparatus by the chlorine gas the maximal dose was limited to 120×10^{-6} torrsec. Different exposures of the crystals were achieved by varying the time t .

In order to apply higher doses of chlorine for adsorption and threedimensional epitaxy and for

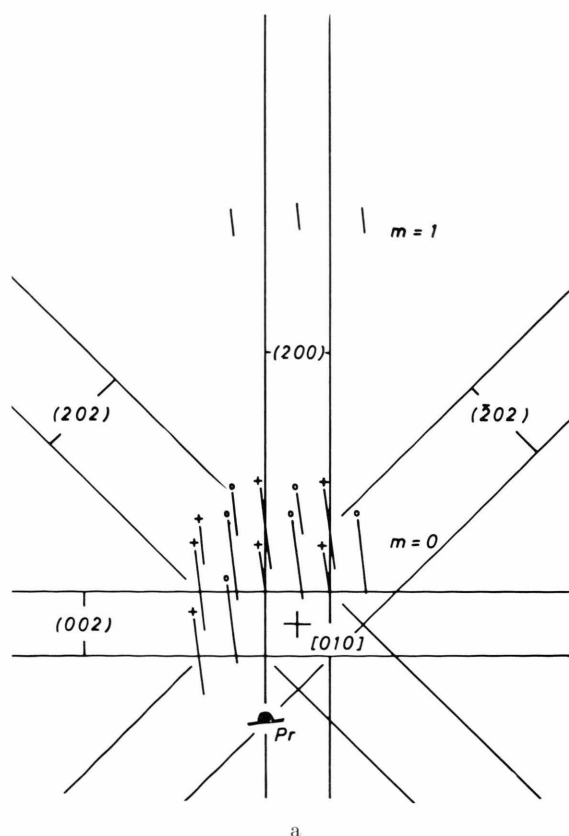


Fig. 2. RHEED diagram from Ag (\approx 018)-Cl. Primary beam nearly parallel to Ag [010]. +: Ag streaks. o: additional streaks from Ag (001) c (2×2)-Cl.

first orientations similar experiments were performed in an older RHEED apparatus with 10^{-5} torr as base pressure ("HV"). Here the diffraction diagrams were recorded photographically inside the apparatus and the pressure of chlorine or of the gases desorbed by chlorine was measured by a Penning gauge.

6. Observed Structures

6.1. $Ag(001) c(2 \times 2)\text{-Cl}$ and $Ag(001) [1\bar{1}0]//AgCl(001) [100]$

After exposure to 60×10^{-6} torrsec of chlorine, streaks of the net $Ag(001) c(2 \times 2)$ appeared. In UHV experiments these streaks were sharper and brighter than in HV experiments. That indicates larger coherent islands for the adsorption structure grown in lower residual pressure. But also in HV the contrast of the streaks was improved if chlorination proceeded. After 6×10^{-3} torrsec, three-dimensional AgCl was indicated by new diffraction spots.

In all experiments, streaks from $c(2 \times 2)$ appeared first on the $Ag(001)$ pole. Later also vicinal planes in an extended area around (001) produced these streaks. The rim of these areas had an angular distance of about 8° from (001) corresponding to the area where the epitaxial system on $Ag(001)$ was observed in ² and also in the presently reported experiments.

The diagrams from vicinal planes on the [001] (Fig. 2) and on the [110] zone circle indicate a typical reciprocal lattice. As for a general vicinal plane ⁹ it is composed by long rods perpendicular to the vicinal plane and bands corresponding to the net of diffraction centers on the (001) terraces which form the vicinal plane as a relief. The bands are perpendicular to (001), their period corresponds to the (001) $c(2 \times 2)$ net and their width is reciprocal to the number of $c(2 \times 2)$ meshes on one (001) terrace. The diffraction intensity is given by the product of the rods and the bands, so the rods are modulated by the bands.

If the angular distance between the vicinal plane and (001) is increased, the width of one terrace and therefore the number of meshes on it is decreased. For distances larger than 8° the modulation of the rods by the bands is still clearly visible for clean silver crystals, but it is blurred for chlorinated crystals, indicating a low order of $c(2 \times 2)$ on small (001) terraces. We suppose that this low order disturbs also the three-dimensional epitaxy of AgCl outside the indicated areas around $Ag(001)$.

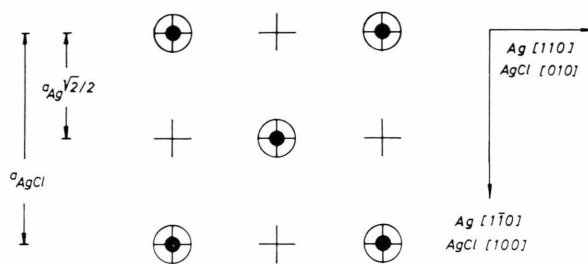


Fig. 3. Correlation between $Ag(001)\text{-Cl}$ structures. $+$: Ag atoms in the substrate surface, \circ : diffraction centers in $Ag(001) c(2 \times 2)\text{-Cl}$, \bullet : Ag or Cl atoms in the contact plane of $Ag(001) [1\bar{1}0]//AgCl(001) [100]$. For misfits see text.

Also inside the rim of this area, but near to it, the order is somewhat reduced; diffusion in the growing epitaxial layer may improve this. This can explain that diffraction spots from AgCl were observed first on this rim.

The adsorbed net $Ag(001) c(2 \times 2)$ correlates well with the contact plane in the epitaxial relation $Ag(001) [1\bar{1}0]//AgCl(001) [100]$. In order to demonstrate this, the nets for both cases are depicted in Figure 3. There is no misfit between the Ag net and the adsorption net. The epitaxial net has a simple misfit F compared with the Ag and the adsorption net. F is defined by $F = (a - a_e)/a$. Sometimes a lower misfit results if one considers the coincidence between the m 'th atom in the substrate and the n 'th atom in the epitaxial layer. $F_{m,n} = (ma - na_e)/ma$. For the epitaxy under discussion $F_{2,1} = 3.9\%$, and between epitaxy and adsorption $F = F_{1,1} = 3.9\%$. Diffraction experiments did not show a continuous transition in F from adsorption to epitaxy.

6.2. $Ag(111) (4/3 \times 4/3)$ and $Ag(111) [0\bar{1}1]//AgCl(111) [0\bar{1}1]$

The tolerated doses for chlorination in the UHV apparatus did not produce superstructures on $Ag(111)$. In experiments starting with a residual pressure of 10^{-5} torr, a chlorine dose of 700×10^{-6} torrsec must be applied in order to produce diffraction diagrams like Figure 4. Similar diagrams were observed on more than 20 crystals in an area around (111) with an angular diameter of 20 to 30° corresponding to the macroscopic terraces around (111).

The reciprocal lattice (Fig. 5) of this superstructure is similar to that of the $Ag(111)$ atomic net with respect to its symmetry. From here the super-net $Ag(111) (4 \times 4)$ can be derived, but without

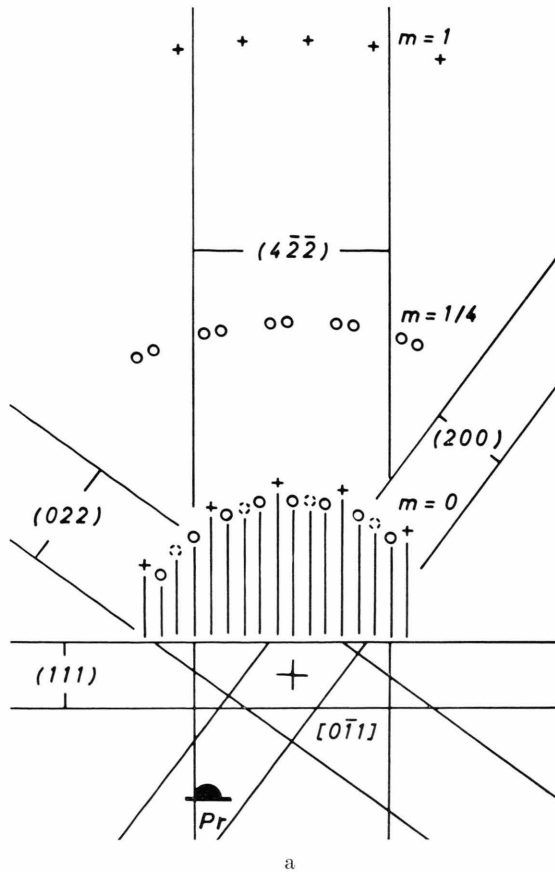


Fig. 4. RHEED diagram from Ag (111) $(4/3 \times 4/3)$ -Cl. Primary beam nearly parallel to $[0\bar{1}1]$. The notation of the Laue circles are in respect to the Ag diagram. +: Ag streaks. o and o: strong and weak additional streaks after chlorination.

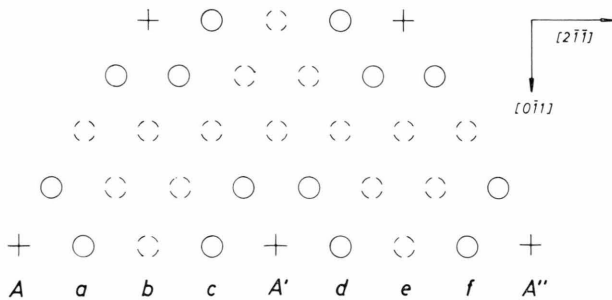


Fig. 5. Reciprocal lattice of Ag (111) $(4/3 \times 4/3)$ -Cl derived from Fig. 4 and others. +: Ag rods. o and o: strong and weak additional rods after chlorination.

considering the observed differences in brightness of the additional streaks. These differences are depicted in Figs. 4 and 5: The streaks from the supernet adjacent to those from the silver net are more intense than the streaks in the middle between the silver streaks. Double diffraction must be assum-

ed: Each silver rod in the reciprocal lattice is a zero beam for diffraction from the supernet, and the distance between one silver rod (A or A' or A'') and six superrods in symmetric position represent the angle of the first diffraction order from the supernet. In Fig. 5 we assume A as the zero order for example; if rod c represents the correct first order of diffraction, the superstructure must be called Ag(111) $(4/3 \times 4/3)$ (Figure 6)¹. This structure is distinguished by its low misfit with respect to the AgCl epitaxy. If rod a is regarded as the first order, the structure (4×4) results and it can be interpreted as the net of coincidence to $(4/3 \times 4/3)$; the second order from (4×4) would be represented by rod b , which was very weak in many experiments. That weakness can be understood in connection with the steep decrease of intensity in electron diffraction as a function of the diffraction angle, if one assumes rod b as the second

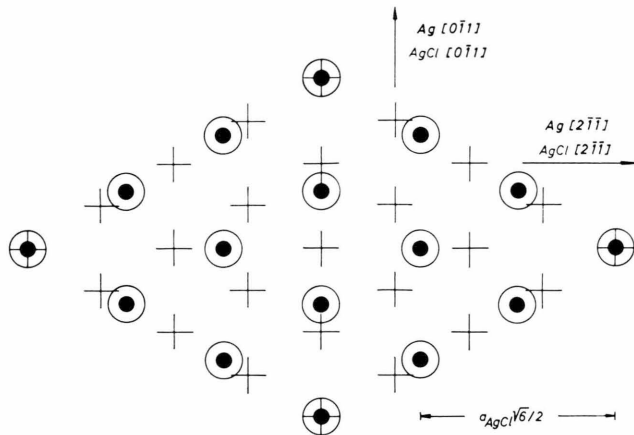


Fig. 6. Correlations between Ag(111)-Cl structures. +: Ag atoms. o: diffraction centers in Ag(111) $(4/3 \times 4/3)$ -Cl. •: Ag or Cl atoms in the contact plane of Ag(111) $[0\bar{1}1] \parallel \text{AgCl}(111) [011]$. For misfit see text.

order from $(4/3 \times 4/3)$ with A'' as the primary beam. Rod d as the first order related to A gives $(4/5 \times 4/5)$, but this structure is not very likely because its period is smaller than the diameter of the chlorine ion. Compared with Ag(001) $c(2 \times 2)$, the streaks from (111) $(4/3 \times 4/3)$ are diffuse, indicating small islands for this structure. Diffraction diagrams from outside the mentioned area around (111) show only the streaks from the Ag vicinal planes.

If chlorination proceeds to a dose of 900×10^{-6} torrsec, three-dimensional epitaxy of AgCl is indicated by pointshaped spots on those intense streaks from $(4/3 \times 4/3)$ which are produced directly without double diffraction. These spots brighten continuously with proceeding chlorination; they indicate the relationship Ag(111) $[0\bar{1}1] \parallel \text{AgCl}(111) [0\bar{1}1]$ (parallel) or Ag(111) $[0\bar{1}1] \parallel \text{AgCl}(111) [01\bar{1}]$ (anti-parallel) as observed in ². The misfit between Ag and AgCl in the contact plane is equal in all directions to the misfit of the lattice constants $F_{1,1} = 36.0\%$. But if one considers a higher coincidence, there is $F_{4,3} = -2.0\%$ ^{1,2}. These multiples correspond to the $(4/3 \times 4/3)$ -Cl structure; this shows the high correlation between adsorption and epitaxy with the low misfit $F_{1,1} = -2.0\%$.

We did not observe the two Ag(111)-Cl structures reported by Rovida et al.⁶. Their structure (3×3) -Cl involves a misfit of 9.4% to the mentioned epitaxial system an Ag(111).

6.3. Adsorption and epitaxy on Ag(011) and near to it on the Ag[100] zone circle

Experiments using UHV and an exposure of 0.1×10^{-6} torrsec of chlorine gas produced diffraction diagrams as shown in Fig. 7 on Ag(011) poles and on vicinal planes near to them. The circle in the diagram, and curved streaks if the primary beam is oblique to $[100]$, indicate parallel planes in the reciprocal lattice which are perpendicular to the Ag $[100]$ directions, their separation is $1/a_{\text{Ag}}$. Therefore a weak adsorption of chlorine produces additional diffraction centers on Ag $[100]$ atomic chains. The period between the centers is equal to the lattice constant a_{Ag} of silver. Because the diffraction diagrams do not show other additional periods, the distances between the $[100]$ chains occupied by Cl diffraction centers must be statistical. The sharpness of the patterns indicate a high number of periods a_{Ag} . These "statistical chains" appear first on the (011) pole. If chlorination proceeds they cover a circular area with a diameter of about 10° around (011). It should be mentioned that in contrast to (001) and (111) no flat areas or terraces were observed in the surrounding of Ag(011).

Surfaces on the $[100]$ zone circle near (011) are vicinal planes to (011), they can be regarded as atomic reliefs consisting of (011) and (001) planes having $[100]$ atomic chains as ledges. If the rectangular net of Ag atoms on a vicinal plane is a primitive one its mesh width is equal to the distances of $[100]$ ledges. If the net is a centered one, the mesh width is twice the ledge distance. After applying a medium chlorination (10×10^{-6} torrsec) the ledges appear to be partially occupied by additional diffraction centers if a vicinal plane between the poles (079) and (012) is under investigation. Electron diffraction with the primary beam perpendicular to $[100]$ shows that the lattice constant a_{Ag} is equal to the distance between the centers of the ledges and it also shows that the distance between these marked ledges are equal to the mentioned mesh widths. All the superstructures mentioned above can be described by Ag($0kl$) (1×1) -Cl. No special vicinal plane is privileged.

If chlorination proceeds to 50×10^{-6} torrsec the area of the "statistical chains" near to (011) becomes ordered. The diffraction diagrams indicate with proceeding chlorination first $2\sqrt{2}a_{\text{Ag}}$ then $(3/2)\sqrt{2}a_{\text{Ag}}$ and finally $\sqrt{2}a_{\text{Ag}}$ as distance between $[100]$ chains corresponding to the surface nets

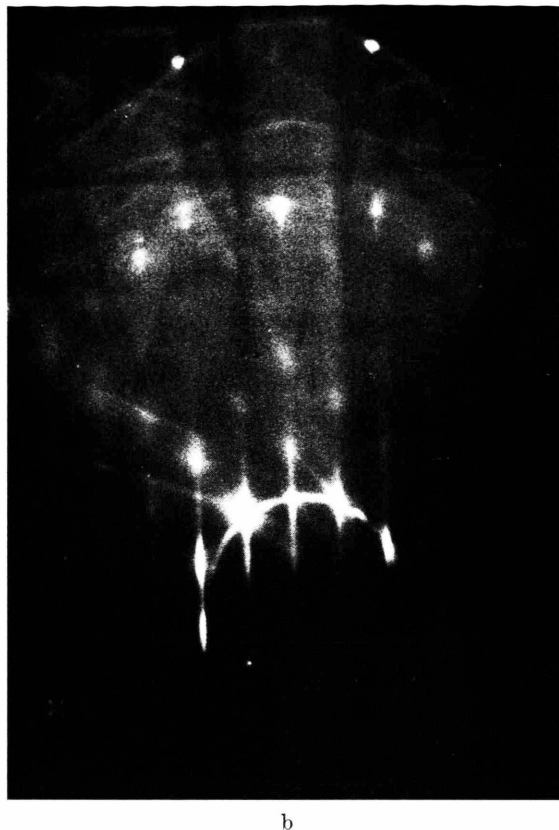
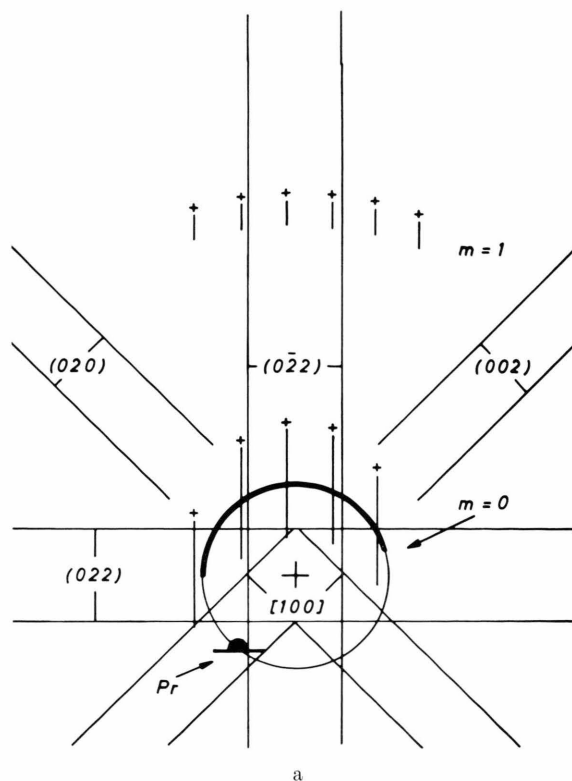


Fig. 7. RHEED diagram from "statistical $\langle 100 \rangle$ chains" on Ag (011) after weak chlorination. Primary beam nearly parallel to $[100]$.

Ag(011) (4×1) , Ag(011) (3×1) and Ag(011) (2×1) . We did not observe a $c(4 \times 2)$ structure as reported by Rovida et al.⁶ after stronger exposition to $C_2H_4Cl_2$.

The Ag(011) (2×1) net was observed without foregoing structures sometimes in UHV if a silver specimen was melted and solidified more than six times and always in the preliminary HV experiments. In these cases chlorination produced first Ag diagrams with an enhanced background, then the (2×1) structure was observed. After chlorination with 500×10^{-6} torrsec this structure was followed by a three-dimensional epitaxy on Ag(012) and advancing to Ag(011) with the relation

$$\text{Ag}(011) [100] \parallel \text{AgCl}(011) [0\bar{1}1]^2.$$

Figure 8 shows the correlation between surface nets belonging to pure Ag, to Ag(011) (2×1) and to epitaxy on Ag(011). The misfit between adsorption and epitaxy in the direction Ag $[100]$ is $F_{1,1}[100] = 3.9\%$ and analogous $F_{2,1}[0\bar{1}1] = 3.9\%$.

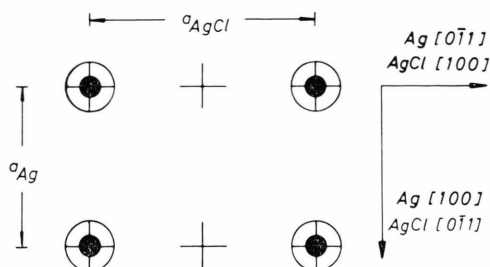


Fig. 8. Correlations between Ag (011)-Cl structures. +: Ag atoms. \circ : diffraction centers in Ag (011) (2×1) -Cl. \bullet : Ag or Cl atoms in the contact 'plane' of Ag (011) $[100] \parallel$ AgCl (011) $[0\bar{1}1]$. For misfit see text.

AgCl crystals grown by epitaxy and observed between the Ag planes (079) and (012) have been shown to be tilted in a systematic way if compared with AgCl on Ag(011)². In² this tilt was related to the net distances both in the Ag vicinal planes and in the AgCl planes in contact with them. As mentioned such a relationship between the Ag nets

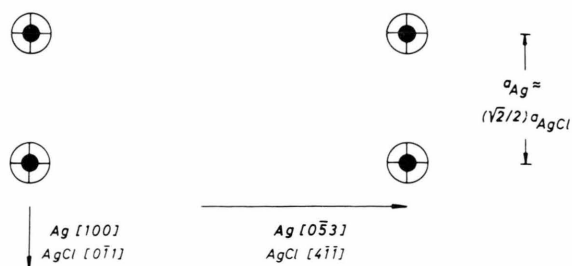


Fig. 9. Example for correlations on Ag (011) vicinal planes: Ag (035). +: Ag atoms. ○: diffraction centers in Ag (035) (1 × 1)-Cl. ●: Ag or Cl atoms in the contact plane of Ag (035) [100]//AgCl (122) [011]. For misfit see text.

of the vicinal planes and the nets after adsorption of Cl was observed in the present investigation. Therefore a correlation between adsorption nets and epitaxial nets is established. Figure 9 depicts the nets on Ag(035) as an example. On this vicinal plane the misfits are $F_{1,1}[100] = 3.9\%$ and $F_{1,1}[053] = 1.1\%$. Following² corresponding correlations can be indicated on the other vicinal planes in the mentioned part of the zone circle.

6.4. Cl adsorption and epitaxy around Ag(011) outside the Ag[100] zone circle

Chlorination on Ag crystals grown at 10^{-9} torr introduces facetting in an area around (011) with an angular diameter of 40° . Only the vicinal planes on the [100] zone circle deviate from this behaviour as described in Chapter 6.3. The facets consist of (011) terraces and probably curved secondary surfaces. On (011) terraces the structure “statistical chains” develop at the beginning of the chlorination, it is followed by (4 × 1) then by (3 × 1) and finally by (2 × 1) as described in Chapter 6.3.

The facetting was derived from diffraction diagrams showing the characteristic streaks of (011) ($n \times 1$) nets together with streaks from the Ag vicinal planes under investigation. These latter streaks are oriented perpendicular to the vicinal plane. Both types of streaks form an angle equal to the angular distance between the vicinal plane and (011). The distances between the vicinal streaks correspond to the periods in the atomically smooth vicinal planes. The sharpness of the (011) ($n \times 1$) streaks indicates extended (011) facets. Facetted areas and smooth vicinal planes must be distributed in islands because both types of streaks appear in the same diffraction diagrams.

If the crystals were grown in a vacuum of 10^{-5} torr chlorination produced in the beginning diffraction diagrams from Ag with reduced contrast. A dose of 300×10^{-6} torrsec of chlorine produced diffuse diagrams corresponding to Ag(011) (2 × 1). These diagrams came from an area with an angular diameter of about 10° . With increasing exposure to chlorine the diagrams became sharper. The angular area around (011) between 10° and 40° produced a strong scattering background. It seems that diffraction centers after chlorination correspond to positions of Ag atoms on the ledges of (011) terraces forming smooth vicinal planes. No facetting seemed to occur in these experiments. For instance, the accentuation of the ledges by chlorination between adsorption and epitaxy of AgCl with the systematic tilt as described in².

6.5. Adsorption near to Ag (013)

Between Ag(079) and (012) structures (0kl) (1 × 1) occurred as was reported in Chapter 6.3. In the adjacent section on the [100] zone circle centered supernets were observed after an exposure of 300×10^{-6} torrsec to chlorine if the crystals were grown in a vacuum of 10^{-5} torr. The mesh width of these supernets in [100] was a_{Ag} and perpendicular to [100] the mesh width was b . The structure Ag(012) c(1 × 3) with $b = 27.10$ Å was observed only occasionally but Ag(025) c(1 × 3) (with $b = 22.00$ Å) and Ag(013) c(1 × 4) (with $b = 25.84$ Å) appeared always. In this area the epitaxial system Ag(013) [100]//AgCl(111) [110] was observed earlier as reported in². The same structure developed here after 500×10^{-6} torrsec of chlorine. Figure 10 shows the nets for pure Ag, the adsorption centers and the epitaxial systems on Ag(013). Between Ag and AgCl the observed misfit were $F_{1,1}[100] = 3.9\%$

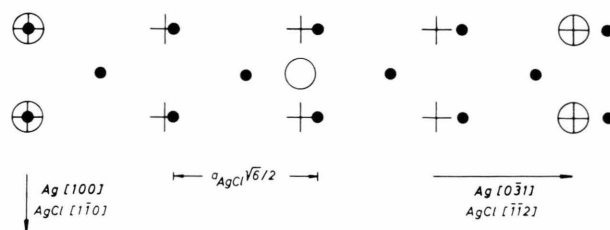


Fig. 10. Correlations between Ag (013)-Cl structures. +: Ag atoms. ○: diffraction centers in Ag (013) c(1 × 4)-Cl. ●: Ag or Cl atoms in the contact plane of Ag (013) [100]//AgCl (111) [110]. For misfit see text.

and $F_{1,1}[\bar{0}\bar{3}1] = -5.3\%$. Between adsorption and epitaxy is a small misfit $F_{1,1}[100] = 3.9\%$ and a large one $F_{1,3}[\bar{0}\bar{3}1] = 21.0\%$. A smaller misfit $F_{1,1}[\bar{0}\bar{3}1] = 0.3\%$ would result for the non observed epitaxy Ag(013) $[100] \parallel \text{AgCl}(533) [0\bar{1}1]$ if the monotonic tilt of AgCl around Ag(011) would extrapolated.

7. Stability of Ag-Cl Adsorption Structures

All the observed structures did not change after storing them in vacuum for several days at a temperature of 20 °C, nor did the electron beam of 30 to 60 keV used for the diffraction experiments effect their stability.

Annealing the adsorption structures in 10^{-9} or 10^{-5} torr and 300 to 400 °C caused the diffraction patterns from the supernets to disappear irrever-

sibly in the background. Annealing Ag(011) (2×1) -Cl in 10^{-9} torr produced the ring from "statistical chains".

After cooling the crystals down, only the patterns from pure silver were observed. The gas analyzer did not detect any peak from chlorine or from its compounds during an annealing process.

Annealing silver crystals with epitaxial AgCl layers was investigated in 10^{-5} torr by taking diffraction diagrams in intervalls at 20 °C. Annealing for a few minutes produced Ag(001) $c(2 \times 2)$ -Cl and Ag(011) (2×1) -Cl as intermediate states. It remains unclear whether Cl is dissolved into the silver or Cl or AgCl are evaporated.

This work was supported by the Deutsche Forschungsgemeinschaft.

- ¹ R. Wilken, Verhandl. DPG (VI) **10**, 570 (1975), Vortrag 0—39.
- ² R. Wilken and E. Menzel, Z. Naturforsch. **28a**, 1914 (1973).
- ³ E. Menzel, Optik **10**, 407 (1953).
- ⁴ E. Menzel, Rept. Progr. Phys. **16**, 47 (1963).

- ⁵ D. W. Pashley, Proc. Roy. Soc. London **A 210**, 354 (1952).
- ⁶ G. Rovida and F. Pratesi, Surf. Sci. **51**, 270 (1975).
- ⁷ E. Zanazzi, F. Jona, D. W. Jepsen, and P. M. Marcus, Phys. Rev. **B 14**, 432 [1976].
- ⁸ E. Menzel, J. Appl. Phys. **35**, 721 [1964].
- ⁹ H. Melle and E. Menzel, Z. Naturforsch. **27a**, 420 [1972].